Available online at www.sciencedirect.com
SCIENCE DIRECT®
C. R. Physique 7 (2006) 187–197
COMPTES RENDUS PHYSIQUE
http://france.elsevier.com/direct/COMREN/

High power fiber lasers and amplifiers/Lasers et amplificateurs à fibre de puissance

Ultrafast high power fiber laser systems

Jens Limpert [a,b,*], Fabian Röser [a], Thomas Schreiber [a], Inka Manek-Hönninger [b], Francois Salin [b], Andreas Tünnermann [a]

[a] *Friedrich Schiller University Jena, Institute of Applied Physics, Albert-Einstein-Strasse 15, 07745 Jena, Germany*
[b] *Celia-Pala, Université Bordeaux 1, 351 cours de la Libération, 33405 Talence, France*

Available online 3 March 2006

Abstract

Fiber laser systems offer unique properties for the amplification of ultrashort pulses to high powers. Two approaches are discussed, the amplification of linearly chirped parabolic pulses and a fiber based chirped pulse amplification system. Using the first method, we succeeded to generate 17-W average power of linearly chirped parabolic pulses at 75 MHz repetition rate and diffraction-limited beam quality in a large-mode-area ytterbium-doped fiber amplifier. The recompression of these pulses with an efficiency of 60% resulted in 80-fs pulses with a peak power of 1.7 MW. Furthermore, we report on a diode-pumped ytterbium-doped double-clad fiber based chirped pulse amplification system delivering 220-fs pulses, at 1040 nm wavelength, 73 MHz repetition rate and up to 131 W average power, corresponding to a peak power of 8 MW. Key element is a diffraction grating compressor consisting of highly efficient transmission gratings in fused silica allowing the recompression at this high power. ***To cite this article: J. Limpert et al., C. R. Physique 7 (2006).***

Résumé

Les systèmes laser à fibre à impulsions ultra-brèves et de forte puissance. Les systèmes de lasers à fibre offrent des propriétés uniques pour l'amplification d'impulsions ultra-brèves. Deux approches sont discutées, l'amplification d'impulsions paraboliques « chirpées » linéairement et une configuration CPA (chirped pulse amplification). En utilisant la première méthode, nous avons obtenu des impulsions paraboliques « chirpées » avec un taux de répétition de 75 MHz, une puissance moyenne de 17 W dans une fibre à large surface de mode et une qualité de faisceau en limite de diffraction. La recompression de ces impulsions, obtenues avec une efficacité de 60%, a produit des impulsions de 80 fs avec une puissance crête de 1,7 MW. Nous présentons, dans un deuxième temps, les résultats obtenus avec une architecture CPA utilisant une fibre double gaine dopée ytterbium qui délivre des impulsions de 220 fs à 1040 nm avec un taux de répétition de 73 MHz. La puissance moyenne atteint 131 W correspondant à une puissance crête de 8 MW. L'élément critique est constitué par un compresseur à réseau de diffraction. Il est composé de réseaux en silice fondue très efficaces en transmission pour la recompression des impulsions à ce niveau élevé de puissance. ***Pour citer cet article : J. Limpert et al., C. R. Physique 7 (2006).***

Keywords: Fiber lasers and amplifiers; Ytterbium; Ultra-short laser pulses; Nonlinear fiber optics

Mots-clés : Amplificateurs et lasers à fibre ; Ytterbium ; Impulsions ultra-brèves ; Effets non-linéaires optiques

* Corresponding author.
E-mail address: jens.limpert@uni-jena.de (J. Limpert).

1631-0705/$ – see front matter
doi:10.1016/j.crhy.2006.01.016

1. Introduction

Today, the development of high repetition rate, high average power femtosecond lasers is pushed by real world applications such as micromaching, which make special demands on the lasers systems regarding pulse duration, pulse energy and repetition rate [1]. Recently, the direct generation of femtosecond laser pulses from passively mode-locked Yb-doped thin disk lasers with average output powers up to several 10 watts has been reported [2,3]. Alternatively to the application of high power laser oscillators, amplifiers can be used to boost up the output of a low power ultrashort pulse oscillator to high average powers. An attractive approach is the application of fiber optical amplifiers.

The first fiber lasers were operated in the beginning of the 1960s at wavelengths around one micron with output powers in the order of a few milliwatts. Owing to recent developments of reliable high brightness all solid state pump sources and the advances in fiber manufacturing technology these devices are no longer restricted to low-power operation. Their main performance advantages compared to conventional bulk solid-state lasers result from the combination of beam confinement and excellent heat dissipation. The generation of high power cw-radiation can be considered as a straightforward problem. Continuous-wave powers of well above 1 kW [4–6] have been achieved with the cladding pump technique [7]. Along with the inherent compactness and stability fiber based systems offer in many fields a significantly higher potential for applications than their bulk solid-state laser counterparts.

Ytterbium-doped fibers provide several key advantages regarding the amplification of short optical pulses. The gain bandwidth supports pulses as short as ∼30 fs, the huge saturation fluence allows the generation of millijoule pulses and the high optical pumping efficiencies (often greater than 80% [8]), make an ytterbium-doped fiber amplifier to an outstanding gain medium.

However, power and energy scaling of ultrafast single-mode fiber amplifiers is restricted due to nonlinear pulse distortions, which are enforced by the large product of intensity and interaction length inside the fiber core. This limitation can be overcome by sufficient pulse stretching in the time domain and the enlargement of the mode-field diameter of the fiber to reduce the nonlinear effects such as stimulated Raman scattering (SRS) and self-phase modulation (SPM) [9]. The application of this technique leads to a chirped-pulse amplification (CPA) system based on either a low-numerical aperture large-mode-area fiber (LMA) [10], a multimode large-core fiber [11] or microstructured fibers [12], where power scaling is limited by the maximum acceptable phase distortion due to self-phase modulation. Using this technique pulse energies in the range of 100 μJ to 1 mJ at sub-picosecond pulse duration are demonstrated at repetition rates of typically less than 10 kHz [13]. Basically, average powers in the 100 W regime are possible, because there are no limitations in scaling the repetition rate to the MHz range.

On the other hand, the nonlinearity can be used to control the propagation of the pulses in a high power fiber amplifier. If no bandwidth limitation is present the combined interaction of normal dispersion, gain and nonlinearity (self-phase modulation) can create linearly chirped parabolic pulses. The linear chirp can be removed using a grating compressor resulting in high power femtosecond pulses.

In this contribution, we report on two approaches of rare-earth-doped fiber based high power femtosecond pulse generation. In Section 2 the generation of 17-W parabolic pulses at a center wavelength of 1060 nm is described. A diffraction grating compressor based on transmission gratings is applied to remove the linear chirp, resulting in 80-fs pulses with 10.2-W average power. Complete spectral and temporal analysis is carried out using numerical simulations, where excellent agreement with the experimental results is achieved. Section 3 discusses a large-mode-area ytterbium-doped fiber based chirped-pulse amplification system which generates 131 W of average power in a diffraction-limited beam. These pulses are recompressed to 220-fs pulse duration applying a novel type of transmission gratings in fused silica. Section 4 is devoted to power and energy scaling potential by employing novel fiber designs. Finally, we give a short summary in Section 5.

2. Fiber based amplification of parabolic pulses

The propagation of high peak power optical pulses in fibers is determined by restricting nonlinear effects, which are enforced by the large product of intensity and interaction length inside the fiber core. Nevertheless, the nonlinearity during the propagation of optical pulses in a high power fiber amplifier can even be used to overcome this limitation. The numerical investigation of the nonlinear Schrödinger equation (NLSE) with gain, which is given by

$$\mathrm{i}\frac{\partial A}{\partial z} = \frac{1}{2}\beta_2\frac{\partial^2 A}{\partial T^2} - \gamma|A|^2 A + \mathrm{i}\frac{g}{2}A \tag{1}$$

reveals that the interplay of normal dispersion, nonlinearity (self-phase modulation) and gain produces a linearly chirped pulse with a parabolic shape, which resists optical wave breaking [14,15]. The linear chirp can be efficiently removed, allowing high-quality pulse compression. In Eq. (1) $A(z, T)$ is the slowly varying pulse envelope in a retarded time frame, β_2 is the group-velocity-dispersion parameter, γ is the nonlinearity parameter and g is the gain coefficient. For an amplifier with constant distributed gain, an exact asymptotic solution has been found that corresponds to a parabolic pulse that propagates self-similar [16]. The asymptotic pulse characteristics are not influenced by the shape or width of the input pulse. Only the initial pulse energy determines the final pulse amplitude and width.

We numerically analyze the NLSE using the standard split-step Fourier method [9]. Fig. 1 shows the spectral and temporal evolution of a Gaussian input pulse at 1060 nm center wavelength with realistic parameters of a 10-m long ytterbium-doped fiber amplifier. The initial pulses have a duration of $\Delta T_0 = 500$ fs and energy $E_i = 400$ pJ. The fiber amplifier provides a gain of 30 dB ($g = 0.7\ \mathrm{m}^{-1}$), $\beta_2 = 0.02\ \mathrm{ps}^2\,\mathrm{m}^{-1}$, and $\gamma = 5.0 \cdot 10^{-4}\ \mathrm{W}^{-1}\,\mathrm{m}^{-1}$. The final parabolic pulses have a pulse duration (FWHM) of 6.7 ps and a spectral width of 49.3 nm, corresponding to a time-bandwidth product of 84.6.

Since the experimental demonstration of self-similar parabolic pulse propagation and amplification in optical fibers [17] the generation of 100-fs pulses with an average power of 5.0 W (13 W before compression) is reported. Even pulses durations as shorts as 52-fs at low average output powers are achieved applying Yb-doped fiber based parabolic pulse amplification and additional third-order dispersion compensation [18].

The experimental setup of our high-power femtosecond fiber amplifier system is shown in Fig. 2. The system consists of a passively mode-locked, diode-pumped solid-state laser system, a diode-pumped ytterbium-doped fiber amplifier and a diffraction-grating compressor based on transmission gratings.

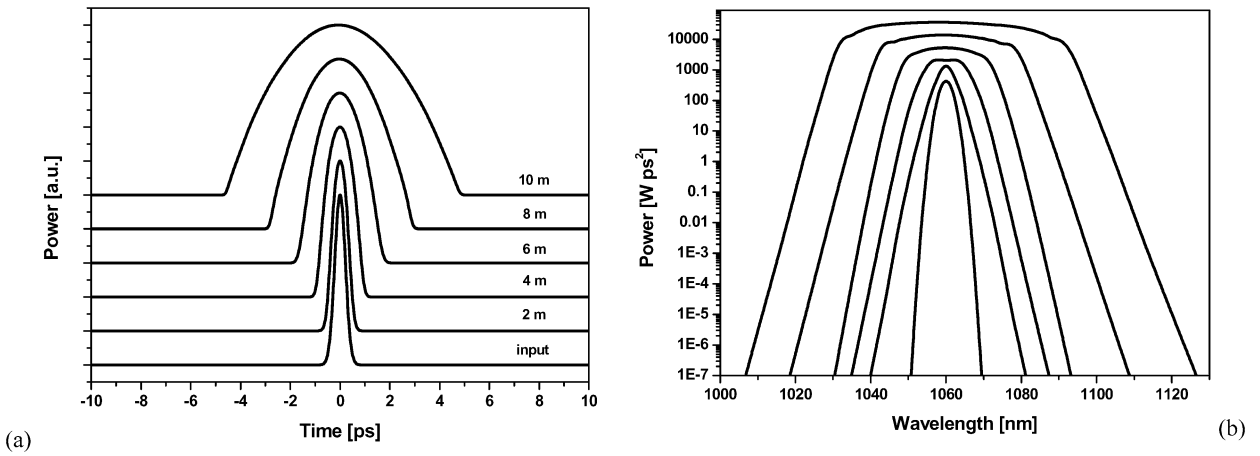

Fig. 1. Evolution of a Gaussian input pulse towards a parabolic output pulse in a 10-m normal-dispersion fiber amplifier; Intensity in the (a) time domain in a linear scale and (b) spectral domain in 2-m increments in a logarithmic scale.

Fig. 1. Évolution d'une impulsion gaussienne en entrée vers une impulsion parabolique en sortie dans un amplificateur à fibre de 10 m en dispersion normale ; Intensité dans (a) le domaine temporel en échelle linéaire et (b) le domaine spectral en échelle logarithmique avec un incrément de 2 m.

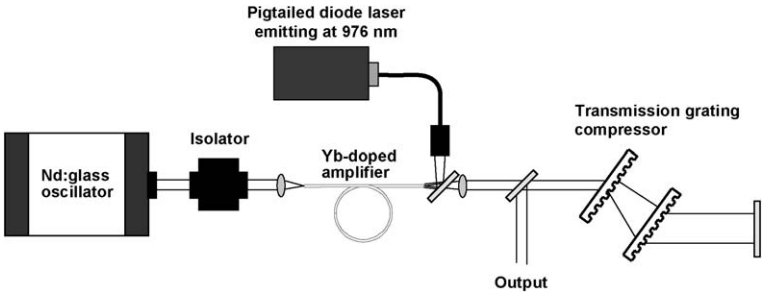

Fig. 2. Experimental setup of the parabolic pulse fiber amplifier.

Fig. 2. Dispositif expérimental d'un amplificateur à fibre d'impulsions paraboliques.

As a femtosecond seed source a Nd:glass laser system is applied, which is based on a semiconductor saturable absorber mirror. The laser is running at 75 MHz repetition rate, producing pulses as short as 180 fs at ∼1060 nm center wavelength and an average power of 100 mW. An optical isolator is used to avoid feedback from the high power fiber amplifier in the oscillator. The high power amplifier is constructed using 9-m length of low-NA large-mode-area fiber with a 30-μm diameter, 0.06-NA step-index ytterbium-doped core, a 400-μm D-shaped inner cladding with NA = 0.38. The ytterbium doping concentration is 500 ppm (mol) Yb_2O_3. The calculated mode-field-diameter of the fundamental mode in this fiber is about 23 μm. This fiber has a V-parameter of about 5 and supports 4 transverse modes. However, coiling the fiber in a radius of less than 10 cm the bending losses discriminate the higher-order transversal mode and only the fundamental mode is guided and amplified. We measured a M^2-value of 1.1 at highest output power. As pump source a pigtailed diode-laser emitting at 976 nm is employed.

Seeding the power amplifier fiber with 10 mW of femtosecond pulses from the Nd:glass oscillator enables us to produce up to 20 W average output power. The slope efficiency is 63% with respect to the absorbed pump power (shown in Fig. 3).

The combined action of gain, nonlinearity and normal dispersion ensures the generation of linearly chirped parabolic pulses which experience large temporal and spectral broadening (see Fig. 1). Fig. 4 shows the measured autocorrelation trace of the output pulses at 17 W average output power. The pulses possess an autocorrelation width

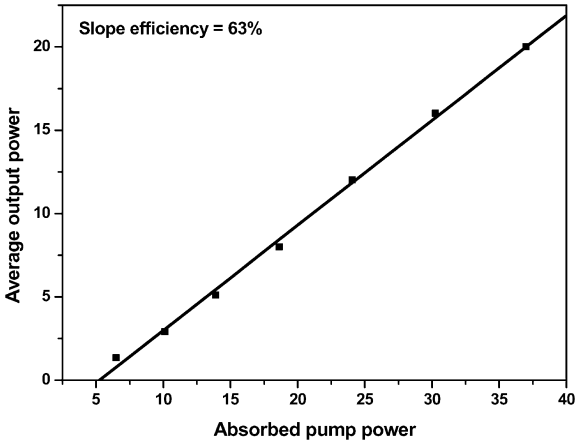

Fig. 3. Output power characteristics of the large-mode-area fiber based amplifier.

Fig. 3. Evolution de la puissance de sortie d'un amplificateur à fibre à large surface de mode.

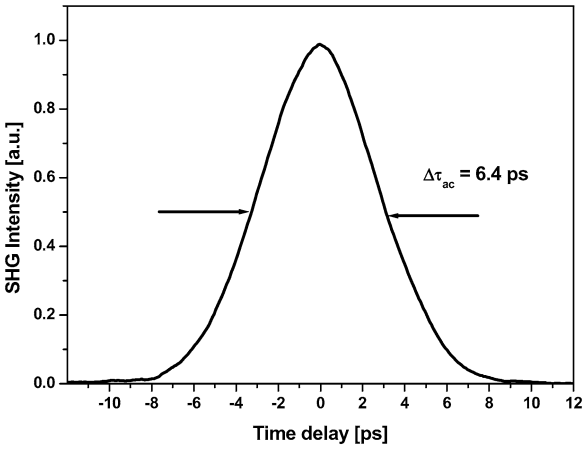

Fig. 4. Measured autocorrelation trace of the output pulses from the fiber amplifier.

Fig. 4. Autocorrélation mesurée des impulsions en sortie de l'amplificateur à fibre.

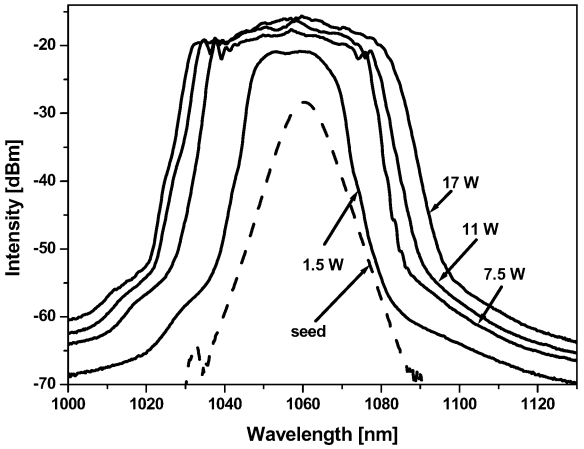

Fig. 5. Experimentally obtained output spectrum of the fiber amplifier.

Fig. 5. Spectre obtenu expérimentalement en sortie de l'amplificateur à fibre.

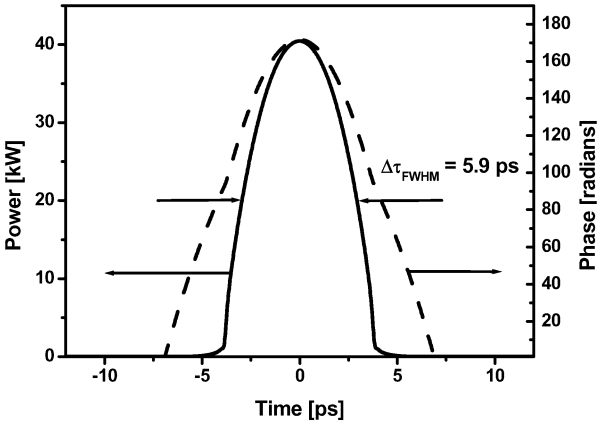

Fig. 6. Calculated pulse shape and temporal phase of the parabolic pulses.

Fig. 6. Profil d'intensité et phase temporelle calculées des impulsions paraboliques.

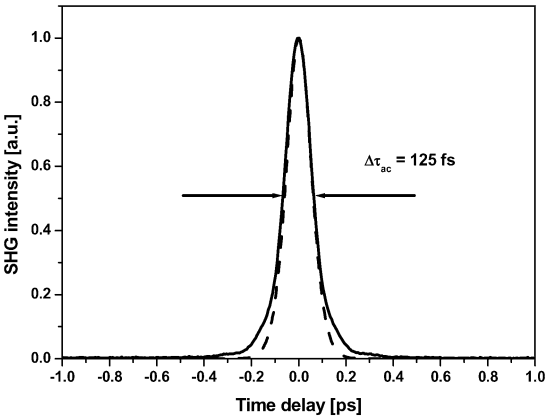

Fig. 7. Intensity autocorrelation trace of the recompressed 80-fs pulses (dashed curve: fit).

Fig. 7. Autocorrelation en intensité des impulsions de 80 fs recompressées (pointillés : approximation analytique).

of 6.4 ps corresponding to a pulse duration of 5.6 ps assuming a parabolic shape. The spectral broadening in the parabolic amplifier is illustrated in Fig. 5 showing the emitted spectrum at different output powers in a logarithmic scale. The conversion of the spectrum of the initial hyperbolic secant pulse to the spectrum of a linearly chirped parabolic pulse can be identified. At an average output power of 17 W the spectral width is increased to 40.5 nm, corresponding to a time-bandwidth product of 58.2.

Numerical investigations of the nonlinear Schrödinger equation (NLSE) using the standard split-step Fourier method are carried out to simulate the pulse evolution in the experiment. The comparison with the experimentally measured spectra reveals a good agreement. The simulated spectral width at 17 W average output power (∼230 nJ) is 40.6 nm.

The simulated pulse shape and temporal phase as well as the corresponding autocorrelation trace are shown in Fig. 6 and indicate the parabolic shape of the pulse. The calculated pulse duration is 5.9 ps and the autocorrelation width is 6.8 ps at 17 W average output power of the LMA fiber amplifier. The uncertainty of the knowledge of the nonlinearity and the dispersion parameter of the real fiber amplifier causes the minor deviation from the measured values. Nevertheless, the simulations confirm the experimental results with a good agreement.

Transmission gratings in fused silica are employed to remove the chirped of the high power parabolic pulses. The gratings are used under Littrow angle. Best compression is achieved at a grating separation of 8.5 mm. Fig. 7 shows the measured autocorrelation trace of the recompressed pulses at an output power of 17 W of the fiber amplifier. We determined the FWHM pulse duration, $\tau_p = 80$ fs, by assuming a sech^2 pulse shape, corresponding to a time-bandwidth product of 0.86. The low-intensity wings in the autocorrelation trace have their origin in uncompensated higher-order phase contributions of the fiber amplifier grating compressor setup.

The compressor efficiency in a double pass configuration is as high as 80%, if the gratings are illuminated with TE-polarized light. This corresponds to an experimental diffraction efficiency of a single grating of 95 %. The degree of polarization of the fiber amplifier output is decreased to 63% (at 17 W output power) due to the inherent variation of birefringence in the large-mode-area fiber. Nevertheless, a compressor efficiency of 60% is reached, resulting in an average power of 10.2 W after compression, corresponding to a pulse peak power of 1.7 MW.

3. High average power fiber based chirped pulse amplification

To significantly scale up the average power or pulse energy of fiber laser systems the well-known technique of chirped pulse amplification (CPA) [19] has to be employed. Stretching the pulses in the time domain reduces the pulse peak power and consequently nonlinear pulse distortion can be avoided to a certain extent. In the following sections the achievements and scaling potential of fiber based chirped pulse amplification is discussed.

In a fiber based CPA system, sufficient pulse stretching and the enlargement of the mode-field diameter of the fiber to reduce the peak power and therefore nonlinear effects such as the discussed effects of SRS and SPM are the key points to scale the output parameters. The setup of the state-of-the-art high average power femtosecond fiber laser system [20] is shown in Fig. 8. It consists of a passively mode-locked solid-state laser system, a grating stretcher, a two-stage ytterbium-doped single-mode photonic crystal amplifier and a fused-silica transmission grating compressor.

The femtosecond seed source is a passively mode-locked Yb:KGW laser system producing 150-fs pulses at 73 MHz repetition rate and 1040 nm center wavelength. These pulses are stretched to 120 ps using a conventional gold-coated 1200 lines/mm diffraction grating. The preamplifier and the power amplifier are constructed with air-clad photonic crystal fibers possessing an active core diameter of 40 μm (NA = 0.03) and an inner cladding diameter of 170 μm (NA = 0.62). The used fiber length is just 1.2 m. In the first stage the signal is amplified to 5 W, which is the seed of the power amplifier. The output characteristic of the main amplifier is shown in Fig. 9. Up to 175 W of average power is obtained with a slope efficiency of ∼75% with respect to the launched pump power. The emitted beam quality is nearly diffraction limited ($M^2 < 1.2$).

The stretched and amplified pulses are recompressed using the transmission gratings in fused silica and are almost matched to the grating stretcher by having a period of 1250 lines/mm. Due to the higher average power damage threshold compared to conventional gold-coated diffraction gratings, these gratings are again one of the key elements of the high average power fiber CPA system.

Fig. 10 shows the measured autocorrelation trace at the highest output power of the fiber amplifier. Best compression is achieved at a grating separation of 0.90 m. This optimal grating distance stayed unchanged with increasing power. This means that the influence of nonlinearity can be neglected, which was also confirmed by numerical simulations. The autocorrelation width is determined to be 340 fs corresponding to 220 fs pulse duration (FWHM) assuming

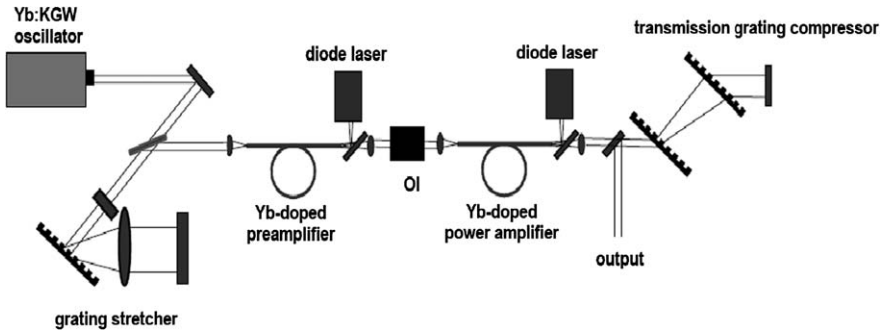

Fig. 8. Schematic setup of the high average power fiber CPA system. OI: optical isolator.

Fig. 8. Représentation schématique d'un système CPA de forte puissance moyenne. OI : isolateur optique.

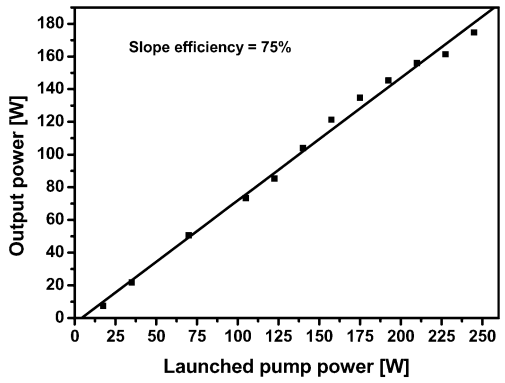

Fig. 9. Output power evolution of the ytterbium-doped fiber power amplifier.

Fig. 9. Evolution de la puissance de sortie d'un amplificateur à fibre dopée ytterbium.

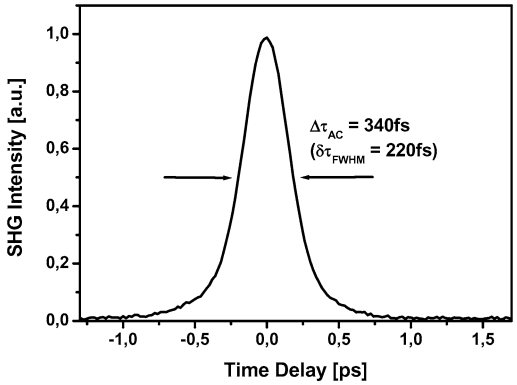

Fig. 10. Measured autocorrelation trace of the high average power femtosecond pulses.

Fig. 10. Autocorrélation mesurée des impulsions femtosecondes de forte puissance moyenne.

a sech^2 pulse shape. The pulse duration is constant over the whole power range, no limitations or pulse quality degradation is observed. The difference in pulse duration between the oscillator and the recompressed pulses is just due to slightly mismatched gratings in the stretcher and compressor. The measured compressor throughput efficiency is $\sim$75% resulting in 131 W average power of femtosecond pulses. The peak power is as high as 8.2 MW. To our knowledge this is the highest average power ever reported for ultrashort pulse solid-state laser systems.

The achieved results were only limited by the available pump power and not by nonlinear pulse distortions, therefore further power scaling is possible even with the current system. The recent demonstration of >1 kW output of a continuous-wave fiber laser with nearly diffraction-limited beam quality endorses this statement. Furthermore, the spectral width of the oscillator is completely supported by the amplifier system and stayed unchanged at about 8 nm at all power levels, therefore, even sub-100 fs pulses are obtainable just by employing an oscillator which delivers shorter pulses.

4. Power and energy scaling by novel low-nonlinearity fiber designs

Basically, as discussed above, the nonlinear effects are proportional to the fiber length and the intensity in the fiber core, and therefore are inversely proportional to the mode-field area of the guided radiation in the fiber. Thus, an enlargement of the mode-field diameter and a reduction of fiber length would help to avoid disturbing nonlinear effects. Using special techniques and fiber designs the mode-field-area of single-transverse mode fiber devices could be significantly increased in the past years. To investigate the modal properties, the normalized frequency V is introduced in Eq. (6). It is related to the effective refractive indices of the core n_C and cladding n_{Clad} of the fiber with a core radius a_{eff}. One can show that a fiber becomes single-mode for $V < 2.405$.

$$V = \frac{2\pi}{\lambda} a_{\mathrm{eff}} \mathrm{NA} = \frac{2\pi}{\lambda} a_{\mathrm{eff}} \sqrt{n_C^2 - n_{\mathrm{Clad}}^2} \tag{2}$$

Thus, one approach to increase the core diameter is to decrease the numerical aperture (NA) at a certain value of V. However, in conventional step-index fibers a reduction in the numerical aperture below a certain limit is not tolerable in terms of propagation losses and precision of core fabrication method. Other fiber designs are based on modified index profiles, which increase the single-mode area by using an outer ring structure. Such large-mode area fibers with up to few 10 μm core diameter and diffraction-limited output could be demonstrated [21]. Preferential gain to the fundamental mode is created by an optimally overlapping rare-earth dopant distribution [22]. This concept can be extended to gain and loss managed multimode fibers to discriminate higher-order modes [23]. Stable fundamental mode propagation over more than 20 m at 1.5 μm wavelength is obtained in a conventional step-index core double-clad fiber with a core diameter of 45 μm with a numerical aperture of 0.13 [24]. In this reference it is stated that the mode-coupling between transversal modes is affected by the cladding diameter and the fiber fabrication process. Thus, for maintaining the fundamental mode it is preferable to use large cladding diameters relative to the core diameters and the high quality MCVD process. Further discrimination of higher-order modes is achieved by a careful optimization of the seed launching conditions and incorporated tapered sections [25] inside the fiber laser or amplifier. Using these techniques the single-mode operation of a 50 μm core (MFD $\sim$ 30 μm) fiber amplifier at 1.06 μm was reported [26].

Over the recent years, the most common employed low-nonlinearity fiber concept is the low-numerical aperture large-mode-area (LMA) fiber. Such a LMA fiber has V-parameters in the range of 5 to 10 and can therefore guide several higher-order transverse modes. However, bending losses can be applied to achieve stable fundamental mode operation of a fiber laser or amplifier [27]. Fig. 11 shows the calculated bending losses for the fundamental and three higher-order modes as a function of bending radius in a 30 μm LMA fiber (NA = 0.06) [28]. This calculation reveals a significant discrimination of higher-order transverse modes. As an example, at a bending radius of 50 mm the induced bending loss for the LP_{01} mode is 0.01 dB/m and for the first higher order mode LP_{11} 52 dB/m. This approximately 5 orders of magnitude difference enforces fundamental mode operation.

However, robust and environmentally stable fundamental mode operation in even larger cores is only possible in a truly single-mode fiber. Therefore, a strictly single-mode fiber with large mode-areas would be a significant achievement. Microstructuring the fiber by including air-holes adds several attractive properties to conventional fibers. These so called photonic crystal fibers (or 'holey fibers') are currently subject of intense research [29]. Solid core photonic crystal fibers consist of a regular array of air-filled holes characterized by the hole diameter d and the pitch Λ (Fig. 12(a)). To describe the modal properties, Eq. (2) can also be used for such one-hole missing PCFs where the

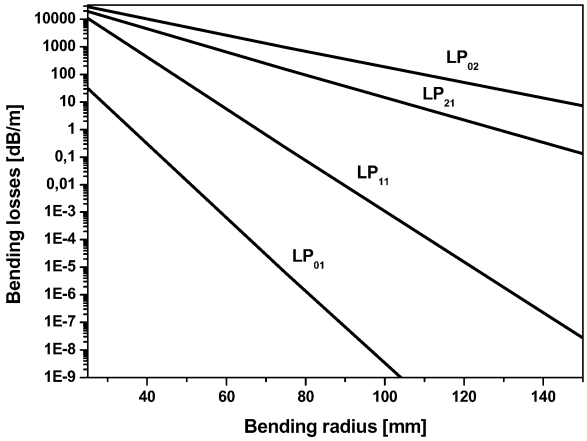

Fig. 11. Calculated bending losses in a 30 μm LMA fiber (NA = 0.06) for the first four transverse modes subject to the bending radius.

Fig. 11. Pertes par courbure calculées dans le cas d'une fibre LMA de 30 μm (NA = 0,06) pour les quatre premiers modes transverses en fonction du rayon de courbure.

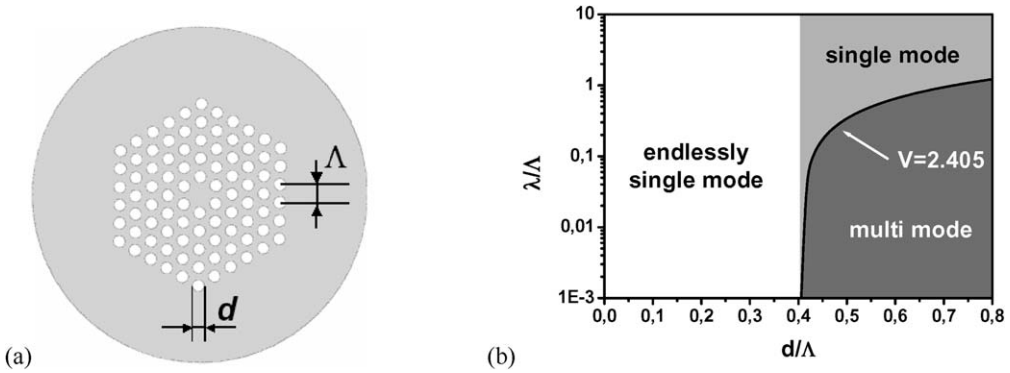

Fig. 12. Structural parameters (a) and modal characteristics of a one hole-missing photonic crystal fiber (b).

Fig. 12. Paramètres structuraux (a) et caractéristiques modales d'une fibre à cristal photonique avec trou central manquant (b).

parameter a_{eff} corresponds to $\Lambda/\sqrt{3}$. The main difference between a standard step index fiber and a PCF is that for PCF the effective cladding index is strongly dependent on λ/Λ. Also, in the limit of $\lambda/\Lambda \to 0$ the effective cladding index reaches the core index. This property becomes more interesting by plotting the single mode boundary $V = 2.405$ of the normalized wavelength over the relative hole diameter as done in Fig. 12(b). For $d/\Lambda > 0.4$ the fiber turns from multi-mode operation into single-mode operation if the relative wavelength is large enough. For $d/\Lambda < 0.4$ the fiber becomes single mode for all wavelengths λ/Λ due to the fact that the wavelength dependence of n_{Clad} keeps the NA low enough to stay single mode. This regime is called endlessly single mode. It was observed in the first photonic crystal fibers and was investigated theoretically soon afterwards [30,31].

Such an endlessly single-mode operation is not known from step index fibers and leads to a concept of scaling the core diameter of a photonic crystal fiber. If the modal properties do not depend on the normalized wavelength λ/Λ, the mode diameter of a PCF, which is proportional to Λ, can theoretically be scaled to infinity at a given wavelength. Of course, the scaling of the core size is limited by increasing propagation losses [32]. If the V-parameter of the photonic-crystal fiber is smaller than one, confinement of the mode is too weak and leakage occurs through a PCFs finite cladding. On the other hand, if the value λ/Λ becomes too small (<0.1), scattering losses due to longitudinal non-uniformities increase, e.g., losses due to micro-bending, macro-bending and dielectric imperfections play an important role. If further scaling of the mode-field diameter is necessary, the core can be extended to consist of more than one missing hole, i.e., three missing holes [33]. Even seven missing hole PCFs are demonstrated with mode field diameters of ∼50 μm and fundamental mode guidance [34].

The gain medium of a fiber laser can be fabricated by replacing the pure silica core by a rare-earth-doped rod. In general, the core is co-doped with fluorine to compensate for the refractive index increase due to the rare-earth

ion. This ensures that the refractive index of the rod closely matches that of the silica cladding. The refractive-index step can be reduced to $\sim 10^{-5}$ even at relatively high ytterbium doping levels, so that the guiding properties are determined by the photonic crystal structure surrounding the core and not by any index step due to the dopants. A further advantage of microstructuring a fiber is the possibility of forming an air-cladding region to create double-clad fibers [35]. Double-clad PCFs can be achieved by surrounding the inner cladding with a web of silica bridges, which are substantially narrower than the wavelength of the guided radiation. The result is a very high numerical aperture of the inner cladding up to 0.8. This allows for reducing the diameter of the inner cladding while maintaining sufficient brightness acceptance for efficient pumping. The advantage of shrinking the inner cladding is that the overlap ratio of the core to the inner cladding increases, leading to shorter absorption lengths and therefore reduced nonlinearity [36,37].

Recently, a fiber design has been developed, which exhibits extremely reduced nonlinearity. This type is called rod-type photonic crystal fiber [38]. The basic idea of this fiber design is to have outer dimensions of a rod laser, meaning a diameter in the range of a few millimeters and a length of just a few tens of centimeters, but including two important waveguide structures, one for pump radiation and one for laser radiation. Finally, such a fiber has an extremely reduced nonlinearity and therefore allows for significant power and energy scaling. The cross-section of this fiber is shown in Fig. 13. The inner cladding has a diameter of $\sim$180 μm. The numerical aperture is as high as 0.6. The ytterbium-doped core has a diameter of 60 μm, to our knowledge this represents the largest single-mode core ever reported for doped fibers. This fiber possesses a pump light absorption as high as $\sim$30 dB/m at 976 nm. Usually, the extraction of high-power levels from short fiber lengths is limited by thermo-optical problems. A detailed analysis of the thermo-optical behavior of high-power fiber lasers (including photonic crystal fibers) has revealed that power scaling is restricted by damage to the polymer coating, which occurs at fiber surface temperatures between 100 and 200 °C [39]. These temperatures are easily reached if power levels in the 100 W/m range are extracted. In a conventional double-clad fiber the coating has an optical function. The coating has to have a lower refractive index than fused silica and therefore forms the waveguide for pump radiation. In contrast, in a microstructured air-clad fiber it just serves to protect the fiber from mechanical damage and chemical attack. The most straightforward way to avoid damage of the coating is to remove it. This can be done if the fiber itself has enough mechanical stability, i.e., if the fiber is thick enough. The fiber shown in Fig. 7 has an outer cladding diameter as large as 2 mm and possesses no coating. In addition, the larger outer diameter improves the heat dissipation capabilities of this fiber [39] and also reduces the propagation loss of weakly guided radiation because of the increased rigidity.

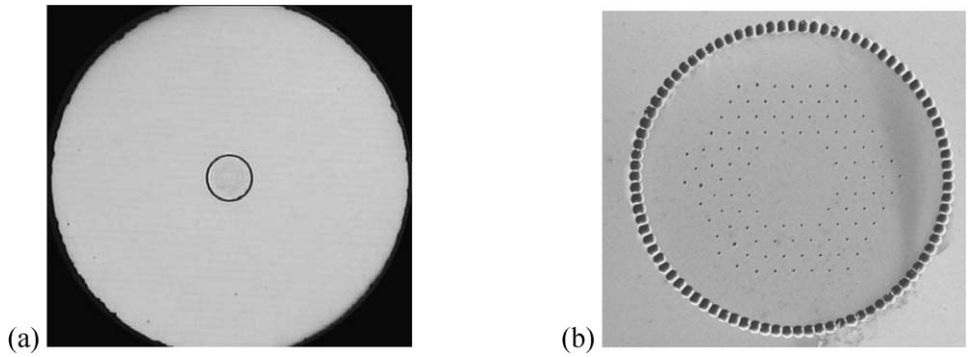

Fig. 13. Microscope image of a rod-type photonic crystal fiber (a) and close-up view of the inner cladding and core regions (b).

Fig. 13. Image au microscope d'une fibre à cristal photonique de type barreau (a) et vue agrandie des zones correspondant à la gaine interne et au coeur (b).

Table 1
Comparison of the nonlinearity in different fiber designs

Tableau 1
Comparaison des nonlinéarités pour différents types de fibres

	Standard step-index fiber	Low-NA LMA fiber	Rod-type PCF
MFD, fiber length	6 μm, 15 m	25 μm, 5 m	50 μm, 0.5 m
$(\text{Nonlinearity})^{-1}$	1	50	2000

A comparison of nonlinearity between a double-clad ytterbium-doped step-index single-mode fiber, a low-numerical large-mode-area fiber and the described single-transverse mode rod-type photonic crystal fiber shows the achievement of this novel fiber design (Table 1). The nonlinearity, basically given by the effective mode area and the absorption length of the fiber, is normalized to the value of the standard single mode step-index fiber in the 1 μm wavelength region. This comparison reveals a reduction of nonlinearity by a factor of about 2000 in the rod-type PCF. As stated above, whenever power or energy scaling is limited by nonlinearity such a fiber offers a significant potential.

References

[1] M.E. Fermann, A. Galvanauskas, G. Sucha, Ultrafast Lasers, Marcel Dekker, New York, 2002.
[2] F. Brunner, T. Südmeyer, E. Innerhofer, R. Paschotta, F. Mourier-Genoud, U. Keller, J. Gao, K. Contag, A. Giesen, V.E. Kisel, V.G. Shcherbitsky, N.V. Kuleshov, 240-fs pulses with 22-W average power from a mode-locked thin-disk Yb:KY(WO4)2 laser, Opt. Lett. 27 (2002) 1162.
[3] E. Innerhofer, T. Südmeyer, F. Brunner, R. Häring, A. Aschwanden, R. Paschotta, C. Hönninger, M. Kumkar, U. Keller, 60-W average power in 810-fs pulses from a thin disk Yb:YAG laser, Opt. Lett. 28 (2003) 367.
[4] Y. Jeong, J.K. Sahu, D.N. Payne, J. Nilsson, Ytterbium-doped large-core fiber laser with 1.36 kW continuous-wave output power, Opt. Express 12 (2004) 6088–6092.
[5] www.ipgphotonics.com.
[6] A. Tünnermann, T. Schreiber, F. Röser, A. Liem, S. Höfer, H. Zellmer, S. Nolte, J. Limpert, The renaissance and bright future of fibre lasers, J. Phys. B: At. Mol. Opt. Phys. 38 (2005) 681–693.
[7] E. Snitzer, H. Po, F. Hakimi, R. Tumminelli, B.C. McCollum, Double-clad, offset core Nd fiber laser, in: Optical Fiber Sensors, in: 1988 OSA Technical Digest Series, vol. 2, Optical Society of America, Washington, DC, 1988, postdeadline paper PD5.
[8] L. Goldberg, J.P. Koplow, D.A.V. Kliner, Highly efficient 4-W Yb-doped fiber amplifier pumped by a broad-strip laser diode, Opt. Lett. 24 (1999) 673.
[9] G.P. Agrawal, Nonlinear Fiber Optics, Academic, San Diego, CA, 1995.
[10] N.G.R. Broderick, H.L. Offerhaus, D.J. Richardson, R.A. Sammut, Power scaling in passively mode-locked large-mode area fiber lasers, IEEE Photon. Technol. Lett. 10 (1998) 1718.
[11] M.E. Fermann, Single-mode excitation of multimode fibers with ultrashort pulses, Opt. Lett. 23 (1) (1998) 52.
[12] J. Limpert, A. Liem, M. Reich, T. Schreiber, S. Nolte, H. Zellmer, A. Tünnermann, J. Broeng, A. Petersson, C. Jakobsen, Low-nonlinearity single-transverse-mode ytterbium-doped photonic crystal fiber amplifier, Opt. Express 12 (2004) 1313–1319.
[13] A. Galvanauskas, Mode-scalable fiber-based chirped pulse amplification systems, IEEE J. Sel. Top. Quantum Electron. 7 (2001) 504–517.
[14] D. Anderson, M. Desaix, M. Karlson, M. Lisak, M.L. Quiroga-Teixeiro, Wave-breaking-free pulses in nonlinear-optical fibers, J. Opt. Soc. Amer. B 10 (1993) 1185.
[15] K. Tamura, M. Nakazawa, Pulse compression by nonlinear pulse evolution with reduced optical wave breaking in erbium-doped fiber amplifiers, Opt. Lett. 21 (1) (1996) 68.
[16] V.I. Kruglov, A.C. Peacock, J.D. Harvey, J.M. Dudley, Self-similar propagation of parabolic pulses in normal-dispersion fiber amplifiers, J. Opt. Soc. Amer. B 19 (2002) 461.
[17] M.E. Fermann, V.I. Kruglov, B.C. Thomson, J.M. Dudley, J.D. Harvey, Self-Similar Propagation and Amplification of Parabolic Pulses in Optical Fibers, Phys. Rev. Lett. 84 (2000) 6010.
[18] M.E. Fermann, M.L. Stock, A. Galvanauskas, G.C. Cho, B.C., Thomson, Third-order dispersion control in ultrafast Yb fiber amplifiers, in: Advanced Solid-State Lasers, in: OSA Trends in Optics and Photonics Series, vol. 50, 2001, p. 355.
[19] D. Strickland, G. Mourou, Compression of amplified chirped optical pulses, Opt. Com. 55 (1985) 447–449.
[20] F. Röser, J. Rothhard, B. Ortac, A. Liem, O. Schmidt, T. Schreiber, J. Limpert, A. Tünnermann, 131 W 220 fs fiber laser system, Opt. Lett. 30 (2005) 2754–2756.
[21] J.A. Alvarez-Chavez, H.L. Offerhaus, J. Nilsson, P.W. Turner, W.A. Clarkson, D.J. Richardson, High-energy, high-power ytterbium-doped Q-switched fiber laser, Opt. Lett. 25 (2000) 37.
[22] J.M. Sousa, O.G. Okhotnikov, Multimode Er-doped fiber for single-transverse-mode amplification, Appl. Phys. Lett. 74 (1999) 1528–1530.
[23] J. Limpert, H. Zellmer, A. Tünnermann, T. Pertsch, F. Lederer, Suppression of higher order modes in a multimode fiber amplifier using efficient gain-loss-management (GLM), Adv. Solid State Lasers 2002, Quebéc City, Canada, paper MB20.
[24] M. Fermann, Single-mode excitation of multimode fibers with ultrashort pulses, Opt. Lett. 23 (1998) 52–54.
[25] J.A. Alvarez-Chavez, A.B. Grudinin, J. Nilsson, P.W. Turner, W.A. Clarkson, Mode selection in high power cladding pumped fibre lasers with tapered section, in: Conference on Lasers and Electro-Optics, OSA Technical Digest, Washington, DC, OSA, 1999, p. 247.
[26] A. Galvanauskas, Mode-scalable fiber-based chirped pulse amplification systems, IEEE J. Sel. Top. Quantum Electron. 7 (2001) 504–517.
[27] P. Koplow, D. Kliner, L. Goldberg, Single-mode operation of a coiled multimode fiber amplifier, Opt. Lett. 25 (2000) 442–444.
[28] J.I. Sakai, T. Kimura, Bending loss of propagation modes in arbitrary-index profile optical fibers, Appl. Opt. 17 (1978) 1499–1506.
[29] J.P. Russell, Photonic crystal fibers, Science 299 (2003) 358–362.
[30] J. Knight, T. Birks, P. Russell, D. Atkin, All-silica single-mode optical fiber with photonic crystal cladding, Opt. Lett. 21 (1996) 1547.
[31] T. Birks, J. Knight, P. Russell, Endlessly single-mode photonic crystal fiber, Opt. Lett. 22 (1997) 961–963.
[32] N.A. Mortensen, J.R. Folkenberg, Low-loss criterion and effective area considerations for photonic crystal fibers, J. Opt. A: Pure Appl. Opt. 5 (2003) 163.

[33] N.A. Mortensen, M.D. Nielsen, J.R. Folkenberg, A. Petersson, H.R. Simonsen, Improved large-mode-area endlessly singlemode photonic crystal fibers, Opt. Lett. 28 (2003) 393.
[34] J. Limpert, A. Liem, T. Schreiber, S. Nolte, H. Zellmer, A. Tünnermann, J. Broeng, A. Petersson, Ch. Jacobsen, H. Simonsen, N.A. Mortensen, Extended large-mode-area single mode microstructured fiber laser, in: Conference on Lasers and Electro-Optics 2004, San Francisco, session CMS.
[35] W.J. Wadsworth, R.M. Percival, G. Bouwmans, J.C. Knight, P.S.J. Russell, High power air-clad photonic crystal fibre laser, Opt. Express 11 (2003) 48–53.
[36] J. Limpert, T. Schreiber, S. Nolte, H. Zellmer, T. Tünnermann, R. Iliew, F. Lederer, J. Broeng, G. Vienne, A. Petersson, C. Jakobsen, High-power air-clad large-mode-area photonic crystal fiber laser, Opt. Express 11 (2003) 818–823.
[37] J. Limpert, A. Liem, M. Reich, T. Schreiber, S. Nolte, H. Zellmer, A. Tünnermann, J. Broeng, A. Petersson, C. Jakobsen, Low-nonlinearity single-transverse-mode ytterbium-doped photonic crystal fiber amplifier, Opt. Express 12 (2004) 1313–1319.
[38] J. Limpert, N. Deguil-Robin, I. Manek-Hönninger, F. Salin, F. Röser, A. Liem, T. Schreiber, S. Nolte, H. Zellmer, A. Tünnermann, J. Broeng, A. Petersson, C. Jakobsen, High-power rod-type photonic crystal fiber laser, Opt. Express 13 (2005) 1055–1058.
[39] J. Limpert, T. Schreiber, A. Liem, S. Nolte, H. Zellmer, T. Peschel, V. Guyenot, A. Tünnermann, Thermo-optical properties of air-clad photonic crystal fiber lasers in high power operation, Opt. Express 11 (2003) 2982–2990.